2011

In the heat of the night - alternative pathway respiration drives thermogenesis in Philodendron bipinnatifidum

Rebecca Miller

N. Grant

L. Giles

Miquel Ribas-Carbo

J. A. Berry

See next page for additional authors

In the heat of the night - alternative pathway respiration drives thermogenesis in Philodendron bipinnatifidum

Abstract

Philodendron bipinnatifidum inflorescences heat up to 42°C and thermoregulate. We investigated whether they generate heat via the cytochrome oxidase pathway uncoupled by uncoupling proteins (pUCPs), or the alternative oxidase (AOX). Contribution of AOX and pUCPs to heating in fertile (FM) and sterile (SM) male florets was determined using a combination of oxygen isotope discrimination, protein and substrate analyses. FM and SM florets thermoregulated independently for up to 30h ex planta. In both floret types, AOX contributed more than 90% of respiratory flux during peak heating. AOX protein increased 5-fold with the onset of thermogenesis in both floret types, whereas pUCP remained low throughout development. These data indicate that AOX is primarily responsible for heating, despite FM and SM florets potentially using different substrates, carbohydrates and lipids, respectively. Measurements of discrimination between O2 isotopes in strongly respiring SM florets were affected by diffusion; however, this diffusional limitation was largely overcome using elevated O2. The first in vivo respiratory flux measurements in an arum show AOX contributes the bulk of heating in P. bipinnatifidum. Fine scale regulation of AOX activity is post translational. We also demonstrate that elevated O2 can aid measurement of respiratory pathway fluxes in dense tissues.

Disciplines

Life Sciences | Physical Sciences and Mathematics | Social and Behavioral Sciences

Publication Details

Miller, R. E., Grant, N. M., Giles, L., Ribas-Carbo, M., Berry, J., Watling, J. R. & Robinson, S. A. (2011). In the heat of the night - alternative pathway respiration drives thermogenesis in Philodendron bipinnatifidum. New Phytologist, 189 (4), 1013-1026.

Authors

Rebecca Miller, N. Grant, L. Giles, Miquel Ribas-Carbo, J. A. Berry, Jennifer Watling, and Sharon A. Robinson

In the heat of the night – alternative pathway respiration drives thermogenesis in *Philodendron bipinnatifidum*

Running title: Alternative oxidase heats *Philodendron*

Rebecca E Miller[1,2,3], Nicole M Grant[1,2], Larry Giles[4], Miquel Ribas-Carbo[5] Joseph A Berry[4], Jennifer R Watling[2] and Sharon A Robinson[1]

[1] *Institute for Conservation Biology and Environmental Management, The University of Wollongong, Wollongong, NSW, 2522, Australia*

[2] *Ecology & Evolutionary Biology, School of Earth and Environmental Sciences, The University of Adelaide, Adelaide, SA, 5005, Australia*

[3] *School of Biological Sciences, Monash University, Clayton, Victoria, 3800, Australia*

[4] *Department of Global Ecology, Carnegie Institution of Washington, 260 Panama St, Stanford, CA 94305, USA*

[5] *Universitat de les Illes Balears, Departament de Biologia, Unitat de Fisiologia Vegetal, Illes Balears, Spain*

Corresponding author: Rebecca E Miller, School of Biological Sciences, Monash University, Clayton, Victoria 3800, Australia. Ph. +61 3 99055217, Email: Rebecca.miller@monash.edu

Word count:

- Body of text: 6500
- Introduction: 924
- Materials & Methods: 1550
- Results: 1974
- Discussion: 1966
- Acknowledgments: 86
- Tables: 2
- Figures: 6

Summary

- *Philodendron bipinnatifidum* inflorescences heat up to 42ºC and thermoregulate. We investigated whether they generate heat via the cytochrome oxidase pathway uncoupled by uncoupling proteins (pUCPs), or the alternative oxidase (AOX).
- Contribution of AOX and pUCPs to heating in fertile (FM) and sterile (SM) male florets was determined using a combination of oxygen isotope discrimination, protein and substrate analyses.
- FM and SM florets thermoregulated independently for up to 30h *ex planta*. In both floret types, AOX contributed more than 90% of respiratory flux during peak heating. AOX protein increased 5-fold with the onset of thermogenesis in both floret types, whereas pUCP remained low throughout development. These data indicate that AOX is primarily responsible for heating, despite FM and SM florets potentially using different substrates, carbohydrates and lipids, respectively. Measurements of discrimination between O_2 isotopes in strongly respiring SM florets were affected by diffusion; however, this diffusional limitation was largely overcome using elevated O_2.
- The first *in vivo* respiratory flux measurements in an arum show AOX contributes the bulk of heating in *P. bipinnatifidum*. Fine scale regulation of AOX activity is post-translational. We also demonstrate that elevated O_2 can aid measurement of respiratory pathway fluxes in dense tissues.

Key Words

Alternative oxidase (AOX), Araceae, diffusion limitation, *Philodendron bipinnatifidum,* plant uncoupling proteins (pUCPs), plant thermogenesis, stable isotope measurements of respiration.

Introduction

Thermogenesis in the reproductive organs of plants is known to occur in the Cycadaceae (Tang *et al.*, 1987), and in Angiosperms, including both eudicots (e.g. Nelumbonaceae; Miyake, 1898) and monocots (e.g. Araceae; Lance, 1974). The Araceae contains more thermogenic species than any other family (Meeuse, 1975; Meeuse & Raskin, 1988; Gibernau *et al*., 2005), and has attracted much attention from researchers aiming to understand heating mechanisms (Wagner *et al.*, 1998; Ito *et al.*, 2003; Crichton *et al.*, 2005; Ito & Seymour, 2005; Onda *et al.*, 2008; Wagner *et al.*, 2008), or to characterise the ecological significance of thermogenesis in plant-pollinator interactions (Gottsberger, 1999; Gibernau & Barabé, 2002). Amongst thermogenic arums, the capacity for heat generation differs markedly, from approximately 1-2°C above ambient temperature in *Monstera obliqua* (Chouteau *et al.*, 2007) to 34°C above in *Philodendron bipinnatifidum* (syn. *P. selloum*; Nagy *et al.*, 1972; Seymour *et al.*, 1983). In addition to this substantial thermogenic capacity, *P. bipinnatifidum* is also noteworthy as one of a small number of thermogenic species that can maintain a relatively constant floral temperature by regulating heat production in response to variations in ambient air temperature (Nagy *et al.*, 1972; Knutson, 1974; Seymour & Schultze-Motel, 1996). Despite the attention they have received, the specific mechanisms of heating and thermoregulation have yet to be determined in the thermogenic Araceae, including *P. bipinnatifidum*.

Respiration using the ubiquitous cytochrome *c* oxidase (COX) pathway is coupled to ATP production. By contrast, in thermogenic plants, heat generation occurs via high respiratory fluxes uncoupled from ATP production, by two possible mechanisms. The first is the alternative pathway of respiration, which branches from the main mitochondrial electron transport chain at ubiquinone and for which the alternative oxidase (AOX) is the terminal oxidase. This pathway bypasses two sites of proton translocation (complexes III and IV), but can still be coupled to electron transport at a third site, complex I. Ubiquitous in plants (Vanlerberghe & McIntosh,

1997), and expressed at high levels in thermogenic tissues (Grant *et al.*, 2008), *AOX* genes are also present in fungi, protists and many animal lineages (McDonald & Vanlerberghe, 2006; McDonald, 2008). The second possible mechanism for heat generation involves plant uncoupling proteins (pUCPs) which act by dissipating the electrochemical gradient, and uncoupling respiratory electron transport from ATP regeneration. Whilst pUCPs are often assumed to only uncouple the COX pathway it is also possible that pUCPs could totally uncouple the AOX pathway to generate maximum heat. Some literature has suggested that substrates utilised can indicate the pathway responsible for heating (Sluse *et al.*, 1998; Ito & Seymour, 2005). Lipids, the major substrate for UCP1 mediated non-shivering thermogenesis in mammalian brown adipose tissue (Lowell & Spiegelman, 2000) are therefore assumed to also be the substrate for pUCPs. Conversely, it is often assumed that the AOX pathway utilises carbohydrate rather than lipid metabolism as free fatty acids have been found to inhibit AOX activity *in vitro* (Sluse *et al.*, 1998).

The only means to definitively demonstrate that AOX is involved in heat production *in vivo* is to quantify alternative pathway flux using stable O_2 isotope discrimination techniques (Ribas-Carbo *et al*., 1995; Day *et al*., 1996). Using this approach with thermoregulatory sacred lotus (*Nelumbo nucifera*), it has been demonstrated that up to 93% of total respiration was via the AOX pathway in heating flowers (Watling *et al.,* 2006; Grant *et al.,* 2008). Subsequent protein and substrate data demonstrated that AOX is solely responsible for heat generation in this eudicot (Grant *et al*., 2008; Grant *et al*., in press). Measurements of respiratory fluxes and discrimination using isotope techniques have not been possible in thermogenic Araceae to date because of the high diffusional resistances in these structurally dense tissues (Guy *et al*., 1989).

The majority of studies of *P. bipinnatifidum* have focused on heating in the band of SM florets (Nagy *et al.*, 1972; Seymour *et al.*, 1984; Seymour, 1999) which are the source of up to 70% of

105 inflorescence heat (Seymour, 1999). Based largely on transcript abundances in different tissues, it
106 has been suggested that pUCPs are the likely mechanism for thermogenesis in SM florets of *P.*
107 *bipinnatifidum* (Ito & Seymour, 2005). Furthermore, a respiratory quotient of 0.83 has been
108 reported for *P. bipinnatifidum* consistent with respiration switching from carbohydrate to lipid
109 metabolism prior to heating (Walker *et al.*, 1983; Seymour *et al.*, 1984) and thus also implicating
110 pUCPs. *AOX* transcripts however, also appeared to increase in heating SM florets of this species
111 (Ito & Seymour, 2005). Importantly transcript abundance is not necessarily correlated with
112 protein abundance or enzyme activity, and expression of AOX and pUCP in non-thermogenic
113 and thermogenic tissues of *P. bipinnatifidum* has not been investigated. Co-expression of both
114 pUCP and AOX proteins has been reported in thermogenic tissues of some other aroids,
115 suggesting the possibility that both may play a role in thermogenesis (Onda *et al*., 2008; Wagner
116 *et al*., 2008).
117
118 This study used *P. bipinnatifidum* as a model for the first *in vivo* measurements of AOX pathway
119 flux during thermogenesis in an arum. Specifically we aimed to investigate whether isotopic
120 discrimination was affected by diffusion during peak respiration in SM florets, by conducting
121 measurements under different O_2 partial pressures. We also characterised heating patterns and
122 mechanisms in the little studied fertile male (FM) florets. Here we present physiological and
123 biochemical data that support a major role for AOX in heating in both SM and FM florets of *P.*
124 *bipinnatifidum in vivo*. We also show how diffusional limitations to discrimination in dense
125 tissues can be largely overcome by measuring stable O_2 isotope discrimination under elevated O_2.
126

Materials and Methods

Plant Material

Philodendron bipinnatifidum Schott ex Endl. (syn. *P. selloum* K.Koch.) spadices were sampled from the Adelaide Botanic Gardens, South Australia, and a private garden in Wollongong, New South Wales during November to December, 2006 and 2007. In Adelaide, spadices were sampled at five of the six developmental stages described below; we were not able to access plants to capture stage D. The entire spadix was removed and transported to the lab in a sealed plastic bag. Spadices were immediately dissected into floret types for respiration measurements, and protein and substrate analyses. Samples for mitochondrial protein analysis were stored on ice, and tissue samples for substrate analysis (lipid, carbohydrate) were snap frozen in liquid N_2 and stored at –80°C until analysed.

Further measurements of respiration and oxygen isotope discrimination were undertaken during the Northern summer, June-July 2009, using plants from private gardens in Palo Alto, California.

Thermogenic stages

Temperatures of SM and FM florets, non-thermogenic spathe tissue, and air were logged every three min, throughout the three to four day flowering period using Thermochron i-Buttons (Maxim Integrated Products, Inc, Sunnyvale, CA). When inflorescences were sampled, air and floret temperatures, including non-thermogenic female florets and spathe temperature, were taken using a needle thermocouple inserted into the florets and a Fluke model 52 digital thermometer (Fluke Corp., Everett, WA, USA). There was no significant difference between i-Button and thermocouple temperatures. Nor were there significant differences between heating of inflorescences in Adelaide, Wollongong or Palo Alto.

Independence of heating in FM and SM florets was assessed by dissecting the spadix into three sections: female florets, FM florets and SM florets. Floret temperatures for each section, and non-thermogenic spathe temperature were logged in the laboratory (RT=approx. 24^{o}C) using i-Buttons over two days.

Several distinct stages were identified, similar to those described in Seymour (1999) based on the heating pattern of the SM florets. The six stages were: pre-thermogenesis (stage A); shoulder (stage B), an initial phase of increasing temperature; peak thermogenesis (stage C), a distinct burst of heating of relatively short duration (< 1 h); the dip (stage D), a sharp decline in temperature after stage C; the plateau (stage E), 8-12 h of relatively constant elevated temperature; and post-thermogenesis (stage F), when heating has ceased after the pollen is shed toward the end of the plateau (Fig. 1).

Respiration and Discrimination Analysis

Oxygen isotope discrimination during respiration of FM and SM florets, at each developmental stage, was determined using the on-line oxygen isotope technique described in Watling *et al.* (2006). The isotopic discrimination factors (D) and partitioning of electrons between the cytochrome and alternative pathways were calculated as previously described (Guy *et al.*, 1989; Henry *et al.*, 1999). The r^2 of all unconstrained linear regressions between –ln f and ln (R/Ro), with a minimum of six data points, was at least 0.992. Discrimination endpoints for the alternative ($\Delta a = 25.6 \pm 1.2‰$; mean ± SD) and cytochrome ($\Delta c = 16.4 \pm 2.9‰$) oxidases were determined (using SM and FM florets incubated with either 16 mM KCN or 25 mM SHAM (in 0.05% DMSO), respectively) and used to calculate flux through the alternative and cytochrome pathways in uninhibited tissues as described in Ribas-Carbo *et al.*, (2005). Female florets are not

thermogenic, and preliminary measurements found very low respiration rates, hence no further analyses were performed.

Because diffusional limitations in dense tissues can influence accurate determination of D, further measurements were made under a range of O_2 partial pressures. Biochemical discrimination during respiration is a function of the ratio of internal to ambient O_2 partial pressures (Pi/Pa) as described by equation 1 (Angert & Luz, 2001).

$$D_{total} = D_d + (D_r - D_d)Pi/Pa \quad (1)$$

Where, D_{total} is the measured discrimination, which is a function of D_d, the discrimination due to diffusion through the tissues (florets), D_r, biochemical discrimination occurring during respiration, and Pi/Pa (i.e. diffusion from air into the tissues). Diffusion through floret tissue is assumed to be in liquid phase, and thus discrimination will be negligible (Farquhar & Lloyd, 1993). Thus, $D_d = 0$ in this case. Equation 1 then simplifies to:

$$D_{total} = D_r*Pi/Pa \quad (2)$$

From Equation 2, it follows that if Pi/Pa is low, then accurate determination of discrimination during respiration will not be possible. To determine whether oxygen isotope fractionation was diffusionally limited during peak heating, we made measurements on stage C, SM florets over a range of O_2 partial pressures, from ambient (21% O_2) to three times ambient (63% O_2) by introducing pure O_2 into the chamber. Mean endpoints for SM florets under elevated O_2 were (Δa = 27.1 ± 1.0‰ and Δc = 18.3 ± 0.5‰; mean ± SD). Measurements in air immediately following those made under increased O_2 supply indicated that there was no oxygen toxicity with total

respiration rates unchanged by O_2 elevation (Supporting Information Fig. S1). These experiments were conducted in Palo Alto.

Isolation of Mitochondrial Proteins

Isolation of washed mitochondrial proteins was based on the method of Day *et al*. (1985). The preparation of mitochondrial proteins, and protein quantification followed methods described in Grant *et al*. (2008). Protein concentrations were determined using the method of Bradford (1976) with known quantities of BSA as standards.

SDS-PAGE and immunoblotting

Mitochondrial proteins separated by SDS-PAGE were transferred to PVDF membranes and detected by chemiluminesence as previously described (Grant *et al*., 2008). Immunoblotting was performed using the mouse monoclonal primary antibodies AOA (1:500, raised against the alternative oxidase of *Sauromatum guttatum* Schott; Elthon *et al*., 1989) and *PM035* from the mitochondrial marker protein porin (1:500, raised against *Zea mays* purified porin protein, Dr T Elthon, Lincoln, NE, USA). The rabbit polyclonal primary antibodies used were anti-COXII (1:1000, raised against subunit II of cytochrome *c* oxidase, Agrisera) and anti-SoyUCP (1:10 000, raised against *Glycine max* L. Merr purified pUCP; Considine *et al*., 2001). For detection of AOX, pUCP and COXII, 60 μg of mitochondrial protein was loaded while only 10 μg was needed for detection of porin. AOX, pUCP and COXII protein levels are given relative to porin which acts as a loading control (Pring *et al*., 2006). The total amount of mitochondrial protein extracted (g^{-1} FW), and porin levels were similar across all developmental stages in all florets (data not shown). The AOX protein was present in the reduced and oxidised form; therefore mitochondrial isolates were incubated in the presence of 5mM DTT to completely reduce the protein. Serial dilutions confirmed linearity of the response of all proteins. Chemiluminescence

(SuperSignal West Femto Maximum Sensitivity Substrate; Pierce, Rockford, IL, USA) was used for the detection of the horse radish peroxidise-conjugated secondary antibodies. Densitometry quantification of the protein bands was made by a Fluorchem 8900 Gel Imager (Alpha Innotech, San Leandro, CA) with subsequent analysis using Fluorchem IS-8900 software (Alpha Innotech, San Leandro, CA).

Soluble carbohydrate and starch determination

Philodendron bipinnatifidum florets from each stage were assayed for soluble carbohydrates and starch as described in Grant *et al*. (2008). Briefly, soluble carbohydrates were extracted by heating florets (mean 0.023 g FW) in 80% ethanol (solvent:tissue, 30:1, v/w) at 70ºC for 10 min. Glucose (glc), fructose (fru) and sucrose (suc) were determined sequentially following the addition of hexokinase (0.5U; Roche 1426362), phosphoglucose isomerase (0.6U; Roche 127396) and invertase (8U; Sigma I-4504), respectively. Absorbance was measured at 340 nm using a SpectraMax Plus 384 microplate reader (Molecular Devices, Sunnyvale, CA). Starch was determined from the remaining tissue, which was ground in H_2O, autoclaved, and incubated with α-amylase (20U; Sigma A-3176) and amyloglucosidase (14U; Fluka 10115) at 37ºC for 4.5 h to convert starch to glc. An aliquot was then assayed for glc as described above.

Lipid analysis

Total lipid was extracted from 0.4 g of frozen floret tissue using standard methods (Folch *et al*., 1957) with minor changes as described. The frozen tissue was ground to a fine powder in liquid N_2 using a mortar and pestle and further homogenised with 10 ml of chloroform:methanol (2:1, v/v) containing butylated hydroxytoluene (0.01%, w/v) as an antioxidant. The homogenised samples were incubated at 4°C overnight on a rotator. Total lipids were separated into triacylglycerides (TAG - neutral lipids) and phospholipids (PL - charged lipids) by sequential

elution from Sep-Pac silica columns (Waters, Milford, MA) with hexane and ethyl acetate, respectively. Samples were dried at 37°C under N_2 in pre-weighed vials. Fatty acid composition of TAGs was then determined. Samples were trans-methylated using the method of Lepage and Roy (1986). The fatty acid methyl esters were separated by gas-liquid chromatography on a Shimadzu GC 17A (Shimadzu, Sydney, Australia) with a Varian WCOT Fused Silica Column (50 m x 0.25 mm ID, CP7419, Sydney, Australia). Fatty acids were identified using retention times of an external standard (F.A.M.E Supelco, Bellefonte, PA), and quantified against a heneicosanoic acid (21:0) internal standard (Sigma Aldrich, Sydney, Australia).

Statistical Analysis

Changes in respiratory pathways and relative AOX, COXII and pUCP protein with respect to developmental stage and between floret types were investigated by analysis of variance (ANOVA). Where ANOVA revealed significant differences, Tukey HSD post hoc tests were applied in order to identify significantly different means. Data were tested for normality using the Shapiro-Wilk W Test. Bartlett's test was applied to ensure homogeneity of variances. Where these assumptions were not satisfied, data were square root or cube root transformed before analysis. All analyses were undertaken using JMP 5.1 (SAS Institute Inc.).

Results

Characterisation of thermogenesis

The pattern of heating for SM florets was similar to that reported by Seymour (1999), but we also observed a distinct and independent pattern of heating in the FM florets, that has not previously been reported in *P. bipinnatifidum*. Mean FM floret temperature at peak thermogenesis (stage C) was 5.5°C lower than in SM florets ($t_{26.0}$=8.2, P<0.0001; Table I), but there were no significant

differences in mean temperatures between floret types at other thermogenic stages (Table I). At peak thermogenesis mean FM floret temperature ranged from 34.0 to 38.1°C (35.7 ± 1.4°C, mean ± SD, *n*=14) against ambient temperatures ranging from 15 to 30.2°C. Peak temperatures in SM florets ranged from 37 to 41.5°C (40.1 ± 1.4°C, *n*=14) across the same range of air temperatures. The slope of the linear regression between peak (stage C) temperature and ambient temperature (T_a) in FM florets (FM peak T = 0.18*T_a + 31.1; *P*=0.04) was significantly different from unity (t_{14}=6.7, P<0.05), but similar to zero indicating strong thermoregulation. SM florets also regulated peak temperature; the slope of the SM floret peak temperature versus Ta relationship was 0.14, similar to previously reported values for SM florets (Nagy *et al*., 1972; Seymour *et al*., 1983). Peak temperatures of FM and SM florets were not correlated with either total spadix mass, or the mass of the specific floret types (data not shown). Dip (stage D) temperatures remained above ambient in both SM and FM florets (Table I). FM florets reached their minimum temperature earlier than SM florets, and began to increase earlier to the thermoregulatory plateau (stage E), during which they maintained a mean temperature of 29.0 ± 1.6°C for 8 to 12 h by heating from 2 to 11.1°C above ambient temperature (Fig 1). The period of temperature regulation at stage E was of longer duration in FM florets than SM florets, which maintained a similar mean plateau temperature (28.8 ± 2.2°C; Table I).

SM and FM florets from dissected spadices continued to heat *ex planta* and exhibited the same pattern of heating as intact inflorescences, for up to 30 h after detachment (Fig. 1b,c). When detached late during stage B (5 pm) peak thermogenesis was achieved rapidly, FM and SM florets reaching maxima of 37.7°C and 39.8°C, respectively (Fig. 1b). If florets were sampled earlier during stage B (1 pm), the peak was broader, and maxima lower (33.3°C and 36.7°C for FM and SM florets, respectively; Fig. 1c). All maxima were within the range of peak temperatures recorded for intact spadices (Table I).

Respiratory fluxes

Mean total respiratory flux increased 2.6-fold with the onset of heating in FM florets ($F_{3,21}$=4.2, *P*=0.0200; Fig. 2a). This increase was largely accounted for by the significant 3.8-fold increase in AOX flux from 0.013 ± 0.006 μmol O_2 g FW^{-1} s^{-1} in stage A (pre-thermogenesis) to its maximum mean value of 0.051 ± 0.013 μmol O_2 g FW^{-1} s^{-1} at stage B ($F_{3,21}$=3.4, *P*=0.0421; Fig. 2a). Across the thermogenic stages (B-E), AOX accounted for, on average, between 44.2 and 74.2% of total respiratory flux in FM florets, and the highest proportion of flux via AOX was 92%. Mean COX flux comprised less than 41% of total flux in FM florets across thermogenic stages B-E, and was similar across all developmental stages (Fig. 2a). In FM florets, both discrimination (D; r^2=0.35, *P*=0.0029) and AOX flux (r^2=0.77, *P*<0.0001) were strongly positively correlated with total respiratory flux (data not shown). That high AOX fluxes were measured when total respiration rates were high, suggests that oxygen fractionation in the FM floret tissue was not diffusionally limited, or that any limitation was minimal.

As stage C is brief, it is possible that inflorescences were sampled after peak temperature had been reached and it appears that peak fluxes in FM florets were not captured (cf. Fig. 2a & 2b), thus relationships between fluxes and heating in these florets were analysed excluding stage C samples. Total respiratory flux (flux=0.0074*heating+0.016, r^2=0.55, *P*=0.0007; Fig. 3a) and AOX flux (flux=0.0062*heating+0.0022, r^2=0.60, *P*=0.0003; Fig. 3c), were significantly positively correlated with heating in FM florets, variation in AOX flux accounting for 60% of the variation in floret heating across all thermogenic stages. Consistent with the absence of substantial changes in COX flux between developmental stages (Fig. 2a), there was no correlation between COX flux and heating in FM florets (Fig. 3c).

Respiratory fluxes in SM florets differed from those in FM florets across the developmental stages (Fig. 2b). Mean total respiratory flux increased significantly with the onset of

thermogenesis ($F_{3,20}$=8.40, *P*=0.0012), and continued to increase to peak thermogenic stage C when the highest respiratory flux in either floret was recorded (0.106 ± 0.013 μmol O_2 g FW^{-1} s^{-1}; Fig. 2b). This suggests that peak fluxes associated with maximum heating in SM florets at stage C were captured (Fig. 2b); thus they were included in regression analysis (Fig. 3b). As in FM florets, there was a significant positive correlation between total respiratory flux and heating in SM florets (flux=0.0060*heating+0.0090, r^2=0.78, *P*<0.0001; Fig. 3b). In contrast, however, apparent AOX flux in SM florets remained low throughout development (Fig. 3d) and was less than one third of the maximum AOX flux recorded in FM florets (0.094 μmol O_2 g FW^{-1} s^{-1}; Fig. 3c).

To investigate whether these apparently low AOX fluxes were a consequence of diffusion influencing discrimination between isotopes (Ribas-Carbo *et al*., 2005) we made measurements during peak heating under a range of O_2 partial pressures. Diffusional limitation to fractionation could occur in dense tissues because of the greater depletion of ^{16}O relative to ^{18}O, leading to a change in the intracellular isotope ratio of the source gas (Guy *et al.*, 1989). These O_2 experiments demonstrated a clear diffusional effect on isotopic discrimination in strongly heating tissues, as total respiratory flux did not increase with increased O_2 supply, however, D values did (Fig. 4 and Table II). In contrast to measurements made in air, where mean AOX fluxes were only 15.7 ± 4.5%, the mean AOX flux in stage C SM florets was 70.8 ± 2.5% under increased O_2 (Table II). We found no evidence of any toxic effects of elevated O_2 on these tissues (Fig. 4; Supporting Information Fig. S1), nor was there any evidence that AOX activity was stimulated by elevated O_2 as: (1) total respiration did not change with O_2 in either floret type (Fig. 4 for SM florets), (2) in SM florets with lower respiration rates, consecutive measures in air and O_2 provided identical low values for both AOX and total respiratory flux, and (3) similarly high AOX fluxes were recorded in both air and elevated O_2 in FM tissues (data not shown). Thus the use of elevated O_2 did not alter the AOX flux, rather it altered our ability to measure AOX flux

accurately, especially in the strongly respiring (heating) stage C florets (Table II; Supporting Information Fig. S1).

As respiration was saturated at 21% O_2 (Fig. 4), increasing O_2 partial pressures will result in an increase in Pi/Pa, thus largely overcoming the diffusional limitation observed at 21% O_2 and enabling more accurate measurement of true discrimination. This is illustrated by the theoretical response of Dt to changes in O_2 concentration, determined using equation 2. In this example, Dr=27.1 (the discrimination endpoint for AOX measured under elevated O_2), and Pi/Pa was determined using Equation 3 across Pa from 0 to 100%.

$$Pi/Pa = (Pa-G)/Pa \quad (3)$$

Where G, the diffusion gradient (Pa-Pi), is a function of the diffusion resistance of the floret tissue (R), and the respiration rate (J), such that G=R*J. We cannot measure R directly, but it was assumed to remain constant, and as there was no change in J as O_2% increased above 21%, G should not change with O_2 (Fig. 4). Therefore, G was adjusted to fit the observed discrimination data, G=7.5% giving the best fit (Fig. 4). While this curve indicates that at Pa above 60% O_2 there will still be some diffusional limitation, it is clear that the error in measuring D at these O_2 concentrations (where Pi/Pa is at least 0.8) is very small, especially relative to biological variation. In addition, this approach provides the possibility of estimating R if Dr is known, and assumed not to change with O_2.

AOX, pUCP, and COXII proteins during thermogenesis

In FM florets, there was a significant 5.4-fold increase in AOX protein (relative to porin) between stages A and B, corresponding with the onset of thermogenesis (Fig. 5a). Subsequently, AOX

levels remained high during the thermogenic stages B-E, and on average decreased by 62% post-thermogenesis between stages E and F, although this was not statistically significant (Fig. 5a). Similarly, the expression of COXII increased significantly (5.1-fold) between stages A and B with the onset of thermogenesis (Fig. 5d). COXII was then maintained at similar levels throughout subsequent developmental stages (Fig. 5d). By contrast, no significant increase in expression of pUCP was detected in FM florets either at the onset of thermogenesis (Fig. 5g), or in subsequent stages. There were no correlations between AOX, COXII or pUCP expression and heating in FM florets (data not shown), nor was there a correlation between AOX content and respiratory flux via the AOX in FM florets (data not shown). This was because levels of these proteins remained constant during stages B-E, while heating varied with changes in ambient temperature. Similarly, neither COXII nor pUCP content correlated with COX flux in FM florets (data not shown).

In SM florets, there was a trend towards increasing AOX with the onset of thermogenesis, and AOX then declined significantly between peak (stage C) and post-thermogenesis (stage F; Fig. 5b). Similarly, there was a significant increase in expression of COXII from pre-thermogenesis to peak (stage C) followed by a significant decline (Fig. 5e). Despite a similar pattern of expression for pUCP, results for this protein were not significant (Fig. 5h). As with FM florets, there were no correlations between AOX, COXII or pUCP expression and heating in SM florets. Similarly, neither pUCP nor COXII protein expressions were correlated with respiratory flux via COX, nor were AOX content and AOX flux correlated (data not shown).

Mitochondrial proteins, AOX, COXII and pUCP (relative to porin), were similar across all stages in female florets (Fig. 5c,f,i). Relative AOX content was significantly lower in female florets (non-thermogenic) than SM and FM florets (2-way ANOVA, $F_{2,7}$=9.9, P=0.002; Fig. 5c). By contrast, relative COXII and pUCP contents were similar across all floret types (Fig. 5).

404

405 *Substrates - carbohydrates and lipids.*

406 Total triacylglyceride (TAG) concentrations were significantly higher in SM florets than FM
407 florets ($F_{1,54}$=23.4, P<0.0001; Fig. 6a,b) particularly across stages A-C. In SM florets, TAG
408 content decreased significantly, by 63%, from peak thermogenesis (stage C) to plateau (stage E;
409 P<0.0001; Fig. 6b). By contrast, in FM florets TAGs remained similar throughout pre-
410 thermogenic and thermogenic stages (A-E), only declining significantly post-thermogenesis once
411 pollen was shed (P=0.0031; Fig. 6a). Total TAG content in both floret types was not significantly
412 correlated with either floret heating or respiratory fluxes across the developmental series (data not
413 shown).

414

415 Conversely, SM florets had significantly lower concentrations of starch than FM florets (2-way
416 ANOVA $F_{1,53}$=27.9, P<0.0001; Fig. 6c,d). Across stages A-E, mean starch concentrations of FM
417 florets (mean ± SE, 5.0 ± 0.6 mg g^{-1} FW) were almost three times greater than SM florets (1.7 ±
418 0.3 mg g^{-1} FW; Fig. 6c,d). Starch content was high in pre-thermogenic FM florets, and remained
419 similar throughout the thermogenic stages, declining significantly by 82% post-thermogenesis
420 (stage F; Fig. 6c). In contrast to FM florets, no significant change in starch content was detected
421 in SM florets across the developmental series (Fig. 6d). Starch content was not significantly
422 correlated with either floret heating or respiratory fluxes across the developmental series (data not
423 shown). Total soluble carbohydrate content of SM and FM florets was similar and did not vary
424 across stages (data not shown).

425

426 ***Discussion***

427 This study has three key findings. First, despite apparently using different fuels, heat production
428 in both fertile and sterile male florets of *P. bipinnatifidum* occurs predominantly via the

alternative pathway. Second, both male floret types can maintain their thermoregulatory activity *ex planta* for up to 30 h. Finally, with the exception of the sacred lotus (Watling *et al*., 2006; Grant *et al*., 2008), measurements of respiratory fluxes and discrimination using isotope techniques have not been possible in other thermogenic tissues to date because of the high diffusional resistances (Guy *et al*., 1989). Our third key finding that diffusional effects on O_2 isotope discrimination in dense tissues can be largely overcome by using elevated O_2 partial pressures provides an important advance in stable isotope measurements of respiration.

Thermogenesis and thermoregulation by fertile male florets

We demonstrated that fertile male (FM) florets heat in a pattern similar to that characterised for sterile male (SM) florets except that FM florets typically commenced heating earlier than SM florets, and had a less pronounced peak and dip than SM florets. Furthermore, measurements of dissected inflorescences in the lab demonstrated that both floret types heat independently.

In the current study, heating in both SM and FM florets lasted for at least 30 h following excision from the plant, and was similar to that recorded on intact inflorescences. This contrasts with previous studies reporting that excision of spadices from *P. bipinnatifidum* stimulates a respiratory burst lasting only 1-2 h, with respiration dropping to very low rates 2 h after removal from the plant (Seymour *et al*., 1983; Seymour, 1991), but is similar to *P. melinonii* where isolated FM and SM florets heated for at least 14 h once cut from the plant (Seymour & Gibernau, 2008). The duration and magnitude of heating in isolated FM and SM florets suggests that all that is required for heat generation (e.g. fuel) and for temperature regulation (e.g. signalling) is contained within the detached inflorescence. Consistent with this, our data indicated that thermogenesis is unlikely to be limited by substrate (lipid or carbohydrate) supply. Calorimetric studies of *P. bipinnatifidum* spadices also concluded that there was no substrate

import into the inflorescence during thermogenesis (Seymour, 1991). In contrast, thermogenesis in other aroids, e.g. *Symplocarpus foetidus* (skunk cabbage) relies on carbohydrate import, and inflorescence heating ceases upon removal from the plant (Knutson, 1974; Ito, *et al.*, 2003).

Mechanisms of heating in P. bipinnatifidum

We identified a clear relationship between *in vivo* alternative pathway (AOX) flux and heating in both FM and SM florets of *P. bipinnatifidum*. Based on our oxygen isotope measurements, the AOX pathway accounts for the bulk of respiratory activity in both of these thermogenic tissues, and indeed the proportions of flux via AOX in SM florets (96%) are the highest measured to date (Ribas-Carbo *et al*., 2005; Watling *et al*., 2006; Grant *et al*., 2008). The high proportions of AOX flux in both FM (up to 92%) and SM florets are similar to those reported in the thermoregulatory receptacles of *N. nucifera* where up to 93% of respiration was via AOX in the most strongly heating flowers, and where AOX flux was strongly correlated with heating (Watling *et al*., 2006; Grant *et al*., 2008). Similarly, 78% of total respiratory flux was via the AOX in isolated mitochondria of thermogenic *Symplocarpus foetidus* (Guy *et al*., 1989). In our study, SM florets, which reach the highest peak temperatures (Table I), also had the highest mean total respiration rate (0.15 μmol O_2 g FW^{-1} s^{-1}; stage C), although peak respiration rates may not have been captured in FM florets (Fig 2a). Given the high proportional engagement of the alternative pathway in *P. bipinnatifidum* thermogenic tissues, fluxes via the AOX are substantial, up to 0.094 μmol O_2 g FW^{-1} s^{-1} and 0.15 μmol O_2 g FW^{-1} s^{-1} in FM and SM florets, respectively.

Our finding that discrimination was essentially the same in FM florets in air or elevated O_2 suggests that diffusional limitations were not an issue with FM florets. In contrast, diffusional limitations to discrimination were observed in SM florets but were essentially overcome by increasing the O_2 concentration, which confirmed that the majority of the respiratory flux in stage

C and E florets is via the AOX pathway. The use of higher O_2 partial pressures to largely mitigate the effects of diffusional limitations to discrimination in these dense tissues opens up the possibility of using stable isotope methodologies not only to measure alternative pathway flux in thermogenic plants, but also in other diffusionally limited tissues. That SM florets displayed O_2 diffusional limitations, but FM florets did not could be a result of the higher total respiration rates in SM florets, and/or be due to differences in floret morphology. For example, FM florets have a higher surface area to volume ratio and thinner cuticle than SM florets (Grant, 2010).

The strong relationship between AOX flux and heating in FM florets, and the substantial proportions of total flux via AOX in both FM and SM florets, suggest there is little room for contribution by pUCPs, except alongside AOX to totally uncouple respiration via concurrent operation of pUCPs and AOX (Onda *et al*., 2008; Wagner *et al*., 2008). If pUCPs alone were responsible for heat generation in *P. bipinnatifidum*, then we would expect an increase in flux through the cytochrome pathway during thermogenesis; however we detected no change in COX flux during heating by FM florets across all thermogenic stages, and comparatively low proportions of total flux via COX in peak heating SM florets when measured under increased O_2 supply. Our protein data further support the substantial role for AOX in thermogenesis in *P. bipinnatifidum*; whereas AOX increases in thermogenic tissues and stages, pUCP does not. Synchronicity between onset of thermogenic activity and the increase in AOX protein in both floret types is similar to the pattern found in sacred lotus (Grant *et al*., 2008), but contrasts with other Araceae (e.g. *Sauromatum guttatum* and *Arum maculatum*) where significant increases in AOX protein precede the onset of thermogenesis by several days (Rhoads & McIntosh, 1992; Chivasa *et al.*, 1999).

Our data provide evidence for developmental regulation of thermogenesis at the level of protein synthesis in *P. bipinnatifidum*; however no significant relationship between AOX protein content and AOX flux was detected during the thermogenic stages. This indicates that fine scale post-translational regulation of AOX activity most likely occurs and is responsible for regulating heat production. Activation of AOX is controlled, in part, by the redox status of the protein which is regulated via the formation of disulfide bonds between conserved cysteine residues (Rhoads *et al*., 1998). At least one isoform of AOX from *P. bipinnatifidum* contains the regulatory cysteines (Ito & Seymour, 2005; Grant *et al.*, 2009); however, around 40% of the protein resists oxidation by diamide (Grant, 2010) suggesting it may lack this redox control. The activity of the reduced protein can be further moderated by effectors such as α-keto acids (e.g. pyruvate, succinate) (Rhoads *et al*., 1998), the specific effector varying depending on the AOX isoform. For example, AOX from thermogenic *N. nucifera* also shows significant redox insensitivity, and stimulation of AOX occurs via succinate rather than pyruvate (Grant *et al*., 2009). An AOX which is not redox regulated (Onda *et al*., 2007; Grant *et al*., 2009) but is controlled by effectors could provide greater control of AOX flux for the precise temperature control these plants achieve over a prolonged period. By contrast, AOX from *Sauromatum guttatum*, which does not thermoregulate but rather heats in a single burst (Meeuse, 1966; Meeuse & Raskin, 1988), is constitutively active (Crichton *et al*., 2005).

The co-occurrence of AOX and pUCP in thermogenic tissues, such as *P. bipinnatifudum,* has raised speculation that both may contribute to heating, but to date there is little evidence that pUCPs function in heat generation in plants (Grant *et al*., 2008; Wagner *et al*., 2008). Based on *pUCP* and *AOX* transcript abundances, the mechanism of thermogenesis in *P. bipinnatifidum* was assumed to be pUCPs (Ito & Seymour, 2005); however, our data clearly demonstrate a predominant role for AOX in heating in this species. Between 70-96% of total flux was via the

alternative pathway in heating FM and SM florets, AOX protein increased specifically in thermogenic male tissues, and no significant difference in amounts of pUCP was found between non-thermogenic and thermogenic stages. If pUCP operated alongside AOX in these tissues we would expect concurrent increases in both proteins throughout thermogenesis. Intriguingly, we did observe an increase in COXII protein with the onset of thermogenesis in both FM and SM florets. Relative amounts, however, were very similar to those observed in non-thermogenic female florets unlike AOX protein which was several fold higher in male as compared to female florets.

Studies indicating that lipids were used as respiratory substrates in thermogenic *P. bipinnatifidum* florets have been used to support a role for pUCPs in thermogenesis in this species (Ito & Seymour, 2005). The assumption derives from the fact that lipids are the substrate for animal UCPs (Argyropoulos & Harper, 2002), and that fatty acids (e.g. linoleic acid) which stimulate pUCP inhibit AOX activity (Sluse *et al*., 1998). Calorimetric studies yielding a respiratory quotient of 0.83, and C isotope analyses suggest that spadices switch from carbohydrate to direct lipid oxidation once the spathe opens and thermogenesis commences (Nagy *et al*., 1972; Walker *et al*., 1983; Seymour *et al*., 1984). We found significant declines in lipid content (total TAGs) towards the end of the thermogenic phase and post-thermogenesis in both SM and FM florets, consistent with lipid oxidation during thermogenesis. In addition, in FM florets, concurrent with the decline in TAGs post-thermogenesis, total starch content also decreased significantly. It is difficult to draw definitive conclusions about the specific substrate for thermogenesis in FM florets because changes in starch and lipids during anthesis may also be associated with maturation of male florets. Nevertheless, the significant decline in starch in FM florets is similar to that recorded in other thermogenic species, including the sacred lotus receptacle (Grant *et al*., 2008), *Symplocarpus foetidus* and *Arum maculatum* (ap Rees *et al*., 1976; ap Rees *et al*., 1977). By contrast, other Araceae may use both lipids and carbohydrates (e.g. *Sauromatum guttatum*;

554 Wilson & Smith, 1971). Our flux and protein data strongly support a role for AOX and
555 demonstrate that AOX and pUCP activity can not be inferred based on substrate type alone. It
556 does seem, however, that lipids are the major substrate for thermogenesis in SM florets of *P.*
557 *bipinnatifidum.* If so, this suggests that AOX activity may not be as sensitive to fatty acids in
558 these tissues as has been observed in non-thermogenic plants such as tomato (Sluse *et al.,* 1998).
559

560 *Conclusion*

561 In summary, we have shown that both sterile and fertile male florets of *P. bipinnatifidum* have
562 independent thermoregulatory phases that persist *ex planta*. Thermogenic activity is driven
563 predominantly via increased flux through the alternative respiratory pathway in both floret types.
564 Whilst increased expression of AOX protein during the thermogenic phase provides the capacity
565 for the increased AOX flux, fine scale regulation of AOX activity must also occur. Although both
566 floret types primarily use the alternative pathway to produce heat, the respiratory fuel appears to
567 differ with lipids and carbohydrates more predominant in SM and FM florets, respectively. A
568 further important finding of this study is that diffusional limitations, that have to date prevented
569 measurements of oxygen fractionation in most thermogenic species, can be mostly overcome, or
570 potentially estimated, as a result of measurement at elevated partial pressures of oxygen. This
571 latter finding provides an important advance to studies aimed at understanding the mechanisms
572 that regulate heating in thermogenic plants, and roles of AOX in dense tissues of non-
573 thermogenic plants. This study clearly demonstrates the importance of functional measurements
574 of respiratory pathways to compliment molecular studies.
575

576 ***Acknowledgments***

577 Thanks are due to the Adelaide and Wollongong Botanic Gardens, Marisa Collins, Ben Licht,
578 Steve Smith and Terry Shuchat for access to *P. bipinnatifidum* plants. Antibodies were kindly

579 donated by Murray Badger (Australian National University, Australia), James Whelan
580 (University of Western Australia, Australia) and Kikukatsu Ito (Iwate University, Japan). Thanks
581 also to Beth Guy for assistance with measurements in California. This work was supported by the
582 Australian Research Council (grant no. DP0451617) and The Hermon Slade Foundation
583 (HSF09/7). NMG received an Australian Postgraduate Award Studentship.

References

Angert A, Luz B. 2001. Fractionation of oxygen isotopes by root respiration: Implications for the isotopic composition of atmospheric O_2. *Geochimica et Cosmochimica Acta* **65**(11): 1695-1701.

ap Rees T, Fuller WA, Wright BW. 1976. Pathways of carbohydrate oxidation during thermogenesis by the spadix of *Arum maculatum. Biochimica et Biophysica Acta* **437**: 22-35.

ap Rees T, Wright BW, Fuller WA. 1977. Measurements of starch breakdown as estimates of glycolysis during thermogenesis by the spadix of *Arum maculatum* L. *Planta* **134**: 53-56.

Argyropoulos G, Harper M-E. 2002. Molecular biology of thermoregulation: Invited review: Uncoupling proteins and thermoregulation. *Journal of Applied Physiology* **92**(5): 2187-2198.

Chivasa S, Berry JO, ap Rees T, Carr JP. 1999. Changes in gene expression during development and thermogenesis in *Arum*. *Australian Journal of Plant Physiology* **26**: 391-399.

Bradford MM. 1976. A rapid and sensitive method for the quantitation of microgram quantities of protein utilizing the principle of protein–dye binding. *Analytical Biochemistry* **72**: 248-254.

Chouteau M, McClure M, Gibernau M. 2007. Pollination ecology of *Monstera obliqua* (Araceae) in French Guiana. *Journal of Tropical Ecology* **23**(05): 607-610.

Considine MJ, Daley DO, Whelan J. 2001. The expression of alternate oxidase and uncoupling protein during fruit ripening in mango. *Plant Physiology* **126**: 1619-1629.

Crichton PG, Affourtit C, Albury MS, Carre JE, Moore AL. 2005. Constitutive activity of *Sauromatum guttatum* alternative oxidase in *Schizosaccharomyces pombe* implicates residues in addition to conserved cysteines in α-keto acid activation. *FEBS Letters* **579**(2): 331-336.

Day DA, Krab K, Lambers H, Moore AL, Siedow JN, Wagner AM, Wiskich JT. 1996. The cyanide-resistant oxidase: To inhibit or not to inhibit, that is the question. *Plant Physiology* **110**: 1-2.

Day DA, Neuburger M, Douce R. 1985. Biochemical characterization of chlorophyll-free mitochondria from pea leaves. *Australian Journal of Plant Physiology* **12**: 219-228.

Elthon TE, Nickels RL, McIntosh L. 1989. Monoclonal antibodies to the alternative oxidase of higher plant mitochondria. *Plant Physiology* **89**(4): 1311-1317.

Farquhar GD, Lloyd J 1993. Carbon and oxygen isotope effects in the exchange of carbon dioxide between terrestrial plants and the atmosphere. In: J. R. Ehleringer, A. E. Hall, G. D. Farquhar eds. *Stable isotopes and plant carbon-water relations*. San Diego: Academic Press, 47-70.

Folch J, Lees M, Sloane-Stanley G. 1957. A simple method for the isolation and purification of total lipids from animal tissue. *Journal of Biological Chemistry* **226**: 497-509.

Gibernau M, Barabé D. 2002. Pollination ecology of *Philodendron squamiferum* (Araceae). *Canadian Journal of Botany* **80**(3): 316-320.

Gibernau M, Barabé D, Moisson M, Trombe A. 2005. Physical constraints on temperature difference in some thermogenic aroid inflorescences. *Annals of Botany* **96**: 117-125.

Gottsberger G. 1999. Pollination and evolution in neotropical Annonaceae. *Plant Species Biology* **14**(2): 143-152.

Grant N, Onda Y, Kakizaki Y, Ito K, Watling J, Robinson S. 2009. Two cys or not two cys? That is the question; alternative oxidase in the thermogenic plant sacred lotus. *Plant Physiology* **150**(2): 987-995.

Grant NM. 2010. *Thermogenesis in plants: The mode of heating and regulation in hot flowers.* PhD thesis, University of Wollongong Wollongong, NSW, Australia.

Grant NM, Miller RE, Watling JR, Robinson SA. 2008. Synchronicity of the thermogenic activity, alternative pathway respiratory flux, AOX protein content, and carbohydrates in receptacle tissues of sacred lotus during floral development. *Journal of Experimental Botany* **59**(3): 705-714.

Grant NM, Miller RE, Watling JR, Robinson SA. in press. Distribution of thermogenic activity in floral tissues of *Nelumbo nucifera. Functional Plant Biology*, in press.

Guy R, Berry JA, Fogel ML, Hoering TC. 1989. Differential fractionation of oxygen isotopes by cyanide-resistant and cyanide-sensitive respiration in plants. *Planta* **177**: 483-491.

Henry B, Atkin OK, Day DA, Millar AH, Menz RI, Farquhar G. 1999. Calculation of the oxygen isotope discrimination factor for studying plant respiration. *Australian Journal of Plant Physiology* **26**: 773-780.

Ito K, Abe Y, Johnston SD, Seymour RS. 2003. Ubiquitous expression of a gene encoding for uncoupling protein isolated from the thermogenic inflorescence of the dead horse arum *Helicodiceros muscivorus*. *Journal of Experimental Botany* **54**(384): 1113-1114.

Ito K, Onda Y, Sato T, Abe Y, Uemura M. 2003. Structural requirements for the perception of ambient temperature signals in homeothermic heat production of skunk cabbage (*Symplocarpus foetidus*). *Plant, Cell and Environment* **26**: 783-788.

Ito K, Seymour R. 2005. Expression of uncoupling protein and alternative oxidase depends on lipid or carbohydrate substrates in thermogenic plants. *Biological Letters* **1**(4): 427-430.

Knutson RM. 1974. Heat production and temperature regulation in eastern skunk cabbage. *Science* **186**: 746-747.

Lance PC. 1974. Respiratory control and oxidative phosphorylation in *Arum maculatum* mitochondria. *Plant Science Letters* **2**: 165-171.

Lepage G, Roy CC. 1986. Direct transesterification of all classes of lipids in a one-step reaction. *Journal of Lipid Research* **27**(1): 114-120.

Lowell BB, Spiegelman BM. 2000. Towards a molecular understanding of adaptive thermogenesis. *Nature* **404**(6778): 652-660.

McDonald AE. 2008. Alternative oxidase: An inter-kingdom perspective on the function and regulation of this broadly distributed 'cyanide-resistant' terminal oxidase. *Functional Plant Biology* **35**: 535-552.

McDonald AE, Vanlerberghe AE. 2006. Origins, evolutionary history, and taxonomic distribution of alternative oxidase and plastoquinol terminal oxidase. *Comparative Biochemistry and Physiology Part D: Genomics and Proteomics* **1**: 357-364.

Meeuse BJ. 1966. The voodoo lily. *Scientific American* **218**: 80-88.

Meeuse BJD. 1975. Thermogenic respiration in aroids. *Annual Review of Plant Physiology and Plant Molecular Biology* **26**: 117-126.

Meeuse BJD, Raskin I. 1988. Sexual reproduction in the arum lily family, with emphasis on thermogenicity. *Sexual Plant Reproduction* **1**: 3-15.

Miyake K. 1898. Some physiological observations on *Nelumbo nucifera*, G. *Botanical Magazine Tokyo* **12**: 112-117.

Nagy KA, Odell DK, Seymour RS. 1972. Temperature regulation by the inflorescence of *Philodendron*. *Science* **178**: 1195-1197.

Onda Y, Kato Y, Abe Y, Ito T, Ito-Inaba Y, Morohashi M, Ito Y, Ichikawa M, Otsuka M, Koiwa H, Ito K. 2007. Pyruvate-sensitive AOX exists as a non-covalently associated dimer in the homeothermic spadix of the skunk cabbage, *Symplocarpus renifolius*. *FEBS Letters* **581**: 5852-5858.

Onda Y, Kato Y, Abe Y, Ito T, Morohashi M, Ito Y, Ichikawa M, Matsukawa K, Kakizaki Y, Kiowa H, Ito K. 2008. Functional coexpression of the mitochondrial alternative

oxidase and uncoupling protein underlies thermoregulation in the thermogenic florets of skunk cabbage. *Plant Physiology* **146**: 636-645.

Pring DR, Tang HV, Chase CD, Siripant MN. 2006. Microspore gene expression associated with cytoplasmic male sterility and fertility restoration in sorghum. *Sexual Plant Reproduction* **19**: 25-35.

Rhoads DM, McIntosh L. 1992. Salicylic acid regulation of respiration in higher plants: Alternative oxidase expression. *Plant Cell* **4**(9): 1131–1139.

Rhoads DM, Umbach AL, Sweet CR, Lennon AM, Rauch GS, Siedow JN. 1998. Regulation of the cyanide-resistant alternative oxidase of plant mitochondria. The identification of the cysteine residue involved in α-keto acid stimulation and intersubunit disulfide bond formation. *Journal of Biological Chemistry* **273**: 30750-30756.

Ribas-Carbo M, Berry JA, Yakir D, Giles L, Robinson SA, Lennon AM, Siedow JN. 1995. Electron partitioning between the cytochrome and alternative pathways in plant mitochondria. *Plant Physiology* **109**: 829-837.

Ribas-Carbo M, Robinson SA, Giles L 2005. The application of the oxygen-isotope techniques to assess respiratory pathway partitioning. In: H. Lambers, M. Ribas-Carbo eds. *Plant respiration: From cell to ecosystem. Advances in photosynthesis and respiration*. Dordrecht: Springer, 31-42.

Seymour RS. 1991. Analysis of heat-production in a thermogenic arum lily, *Philodendron selloum*, by 3 calorimetric methods. *Thermochimica Acta* **193**: 91-97.

Seymour RS. 1999. Pattern of respiration by intact inflorescences of the thermogenic arum lily *Philodendron selloum*. *Journal of Experimental Botany* **50**: 845-852.

Seymour RS. 2001. Diffusion pathway for oxygen into highly thermogenic florets of the arum lily *Philodendron selloum*. *Journal of Experimental Botany* **52**: 1465-1472.

Seymour RS, Barnhart MC, Bartholomew GA. 1984. Respiratory gas exchange during thermogenesis in *Philodendron selloum* Koch. *Planta* **161**: 229-232.

Seymour RS, Bartholomew GA, Barnhart MC. 1983. Respiration and heat production by the inflorescence of *Philodendron selloum* Koch. *Planta* **157**: 336-343.

Seymour RS, Gibernau M. 2008. Respiration of the thermogenic inflorescences of *Philodendron melinonii*: Natural pattern and responses to experimental temperatures. *Journal of Experimental Botany* **59**(6): 1353-1362.

Seymour RS, Schultze-Motel P. 1996. Thermoregulating lotus flowers. *Nature* **383**: 305.

Sluse FE, Almeida AM, Jarmuszkiewicz W, Vercesi AE. 1998. Free fatty acids regulate the uncoupling protein and alternative oxidase activities in plant mitochondria. *FEBS Letters* **433**(3): 237-240.

Tang M, Sternberg L, Price D. 1987. Metabolic aspects of thermogenesis in male cones of five cycad species. *American Journal of Botany* **74**: 1555-1559.

Vanlerberghe GC, McIntosh L. 1997. Alternative oxidase: From gene to function. *Annual Review of Plant Physiology and Plant Molecular Biology* **48**: 703-734.

Wagner AM, Krab K, Wagner MJ, Moore AL. 2008. Regulation of thermogenesis in flowering Araceae: The role of the alternative oxidase. *Biochimica et Biophysica Acta* **1777**(7-8): 993-1000.

Wagner AM, Wagner MJ, Moore AL. 1998. *In vivo* ubiquinone reduction levels during thermogenesis in Araceae. *Plant Physiology* **117**: 1501-1506.

Walker DB, Gysi J, Sternberg L, DeNiro MJ. 1983. Direct respiration of lipids during heat production in the inflorescence of *Philodendron selloum*. *Science* **220**: 419-421.

Watling JR, Robinson SA, Seymour RS. 2006. Contribution of the alternative pathway to respiration during thermogenesis in flowers of the sacred lotus, *Nelumbo nucifera*. *Plant Physiology* **140**(4): 1367-1373.

Wilson RH, Smith BN. 1971. Uncoupling of *Sauromatum* spadix mitochondria as a mechanism of thermogenesis. *Zeitschrift für Pflanzenphysiologie* **65**: 124-129.

Supporting Information

Figure S1. Total respiratory flux and flux via the AOX pathway in sterile male *Philodendron bipinnatifidum* florets; respiration and discrimination were measured sequentially, first in increased oxygen, second in air, and third in increased oxygen.

Figure Legends

Figure 1. Typical temperature traces for sterile and fertile male florets of *Philodendron bipinnatifidum* **(a)** *in planta* and **(b)** excised from the plant**,** and **(c)** photographs of inflorescences at the developmental stages (A-F). In **(a)** temperatures traces are means of three inflorescences logged concurrently shown relative to air temperature over the same two day period. Time is Standard Eastern Australian summer time. Letters indicate thermogenic stages: B shoulder, C peak thermogenesis, D dip, E plateau and F post-thermogenesis. N.B. Stage A pre-thermogenesis not shown. Sunrise was 05:48 and sunset was 19:38. Temperature traces of excised fertile and sterile male florets, and non-thermogenic spathe tissue recorded in the laboratory are from spadices sampled late (5pm) and early (1pm) during stage B.

Figure 2. (a) Total respiratory flux (grey +white) and fluxes through the AOX (white) and COX (grey) pathways by developmental stage in fertile male florets, and **(b)** total respiratory flux by developmental stage in sterile male (SM) florets of *Philodendron bipinnatifidum*. Diffusional limitations in SM florets prevented accurate determination of electron partitioning, thus, only total flux is shown in (b). Developmental stages: A pre-thermogenesis, B shoulder, C peak, E plateau (refer to Fig. 1a for details). Stage C/D: FM peak fluxes were not apparently captured (see Fig. 3a) and samples are likely a mix of stages C and D (dip). Letters indicate significant differences at $P<0.05$. Data are means ± SE of n=4-7 samples.

Figure 3. Relationships between total respiratory flux and heating in **(a)** FM florets and **(b)** SM florets, and between AOX (solid circles) and COX flux (open triangles) and floret heating in **(c)** fertile male florets and **(d)** sterile male florets. Heating was measured as the difference in temperature between FM florets (Tmf) or SM florets (Tsmf), and adjacent non-thermogenic spathe tissue (Tsp). Peak thermogenic stage C FM florets were excluded from correlations for

both **(a)**; total respiration (open circles) and **(c)**; AOX (open circles) and COX fluxes (closed triangles). The regression equations are included in the text. Correlations between COX and AOX fluxes and heating not shown for SM florets due to potential diffusional limitation of isotope fractionation in air.

Figure 4. Theoretical discrimination (Dt; lines) as a function of external O_2 (%) determined from equation 2 and using Dr=27.1 (discrimination endpoint for AOX measured under elevated O_2). Pi/Pa was calculated using Pi/Pa=(Pa-G)/Pa, where G is the diffusion gradient, which was assumed to remain constant as there was no change in respiration rate as O_2 was increased above 21%, as shown by the relative flux rates (closed circles) which vary little from 1 (horizontal line; mean ± SD, 1.0 ± 0.05). Dt response curves are shown for diffusion gradients (G) of 5.0% (solid line), 7.5% (dashed line) or 10% (dotted line). Using G=7.5% gave the best fit for the actual isotopic discrimination data (Dt) for stage C SM florets (open triangles). For Dt measurements, *n*=15 floret samples from 5 inflorescences.

Figure 5. Densitometry results of chemiluminescent signals from western blots of AOX **(a, b, d)**, COXII **(d, e, f)** and pUCP **(g, h, i)** proteins presented relative to Porin in fertile male florets (left panels), sterile male florets (centre panels) and female florets (right panels) of *Philodendron bipinnatifidum* during development. Developmental stages: A pre-thermogenesis, B shoulder, C peak, E plateau, F post-thermogenesis (refer to Fig. 1a for details). Different letters indicate significant differences between stages at $P<0.05$. Data are means ± SE of *n*=3-6 samples.

Figure 6. Changes in total triacylglyceride content **(a, b)**, and starch content **(c, d)** in fertile (left panels) and sterile (right panels) male florets of *Philodendron bipinnatifidum* during development. Developmental stages: A pre-thermogenesis, B shoulder, C peak, E plateau, F

post-thermogenesis (refer to Fig. 1a for details). Different letters indicate significant differences between stages at $P<0.05$. Data are means ± SE of n=4-6 samples.

Table I. Mean floret temperature (± SD, *n*=7-14) and range of heating* for fertile male (FM) and sterile male (SM) florets of attached inflorescences of *P. bipinnatifidum* during development.

		Pre-thermogenic Stage A	Shoulder Stage B	Peak Stage C	Dip Stage D	Plateau Stage E
FM	Temperature (°C)	25.8 ± 6.6	30.3 ± 2.7	35.7 ± 1.4[a]	22.9 ± 2.5	29.0 ± 1.6
Florets	Range (°C)	0.3-2.8	1.2-9.7	5.1-21.0	2.5-8.5	2.0-11.1
SM	Temperature (°C)	24.4 ± 7.3	30.7 ± 1.6	40.1 ± 1.4[b]	22.5 ± 1.9	28.8 ± 2.2
Florets	Range (°C)	0-3.2	2.7-10.6	8.1-26.5	3.5-7.0	1.3-13.9

*Heating was calculated as the difference between floret temperature and temperature of the non-thermogenic spathe tissue.
[a,b] letters indicate a significant difference in peak temperatures between FM and SM florets ($t_{26.0}$=8.19, P<0.0001), no significant differences were found for the other developmental stages.

Table II. Mean proportion and range (%) of total respiratory flux via the alternative pathway (AOX) in *Philodendron bipinnatifidum* sterile male florets during stages C and E, measured in air (*n*=4-5) and in on average 55% O_2 (*n*=3-4).

	Mean proportion of flux via AOX (% ± SE)	Range of flux via AOX (%)	Mean proportion of flux via AOX (% ± SE)	Range of flux via AOX (%)
Stage	Measured in air		Measured in ~55% O_2	
Peak (C)	15.7 ± 4.5	6.7 - 28.0	70.8 ± 2.5	52.3 – 95.5
Plateau (E)	28.9 ± 12.2	0 - 59.6	63.3 ± 5.2	42.0 – 87.5

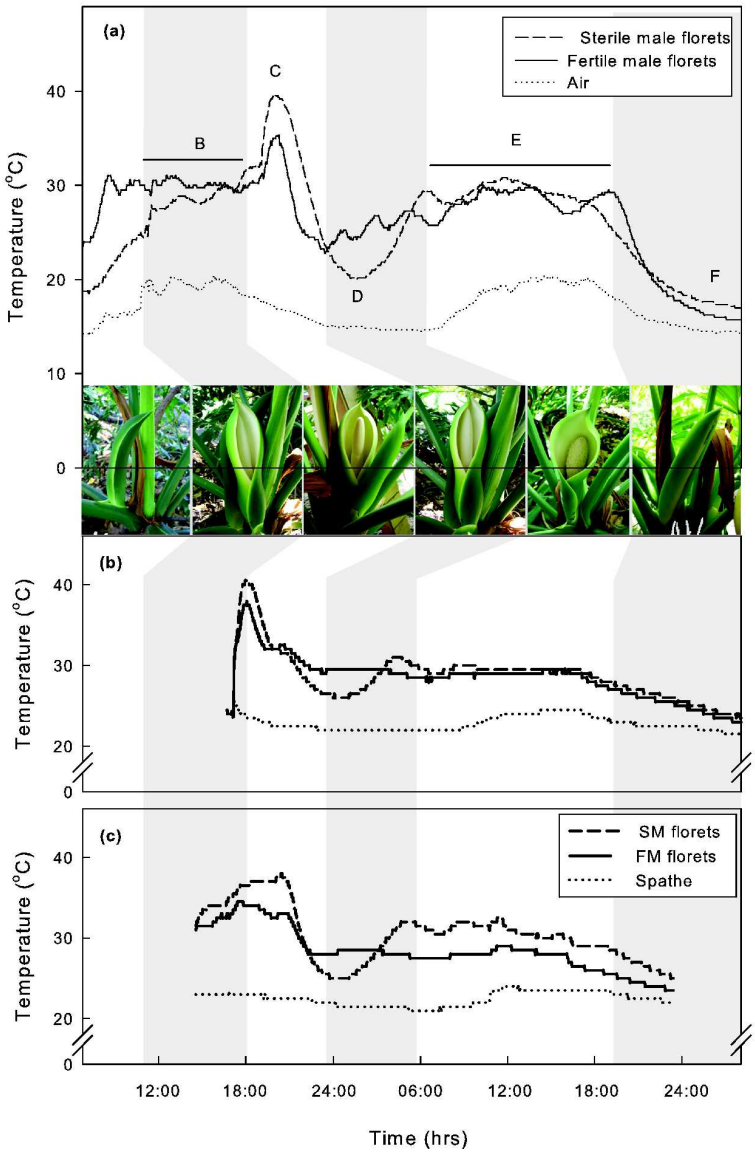

Figure 1. Typical temperature traces for sterile and fertile male florets of Philodendron bipinnatifidum (a) in planta and (b) excised from the plant, and (c) photographs of inflorescences at the developmental stages (A-F). In (a) temperatures traces are means of three inflorescences logged concurrently shown relative to air temperature over the same two day period. Time is Standard Eastern Australian summer time. Letters indicate thermogenic stages: B shoulder, C peak thermogenesis, D dip, E plateau and F post-thermogenesis. N.B. Stage A pre-thermogenesis not shown. Sunrise was 05:48 and sunset was 19:38. Temperature traces of excised fertile and sterile male florets, and non-thermogenic spathe tissue recorded in the laboratory are from spadices sampled late (5pm) and early (1pm) during stage B.
176x251mm (600 x 600 DPI)

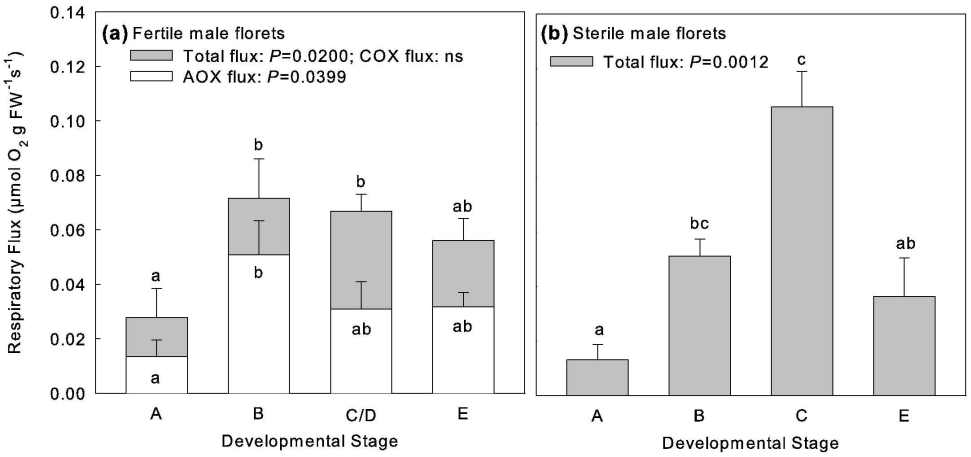

Figure 2. (a) Total respiratory flux (grey +white) and fluxes through the AOX (white) and COX (grey) pathways by developmental stage in fertile male florets, and (b) total respiratory flux by developmental stage in sterile male (SM) florets of Philodendron bipinnatifidum. Diffusional limitations in SM florets prevented accurate determination of electron partitioning, thus, only total flux is shown in (b). Developmental stages: A pre-thermogenesis, B shoulder, C peak, E plateau (refer to Fig. 1a for details). Stage C/D: FM peak fluxes were not apparently captured (see Fig. 3a) and samples are likely a mix of stages C and D (dip). Letters indicate significant differences at $P<0.05$. Data are means ± SE of n=4-7 samples.
189x128mm (600 x 600 DPI)

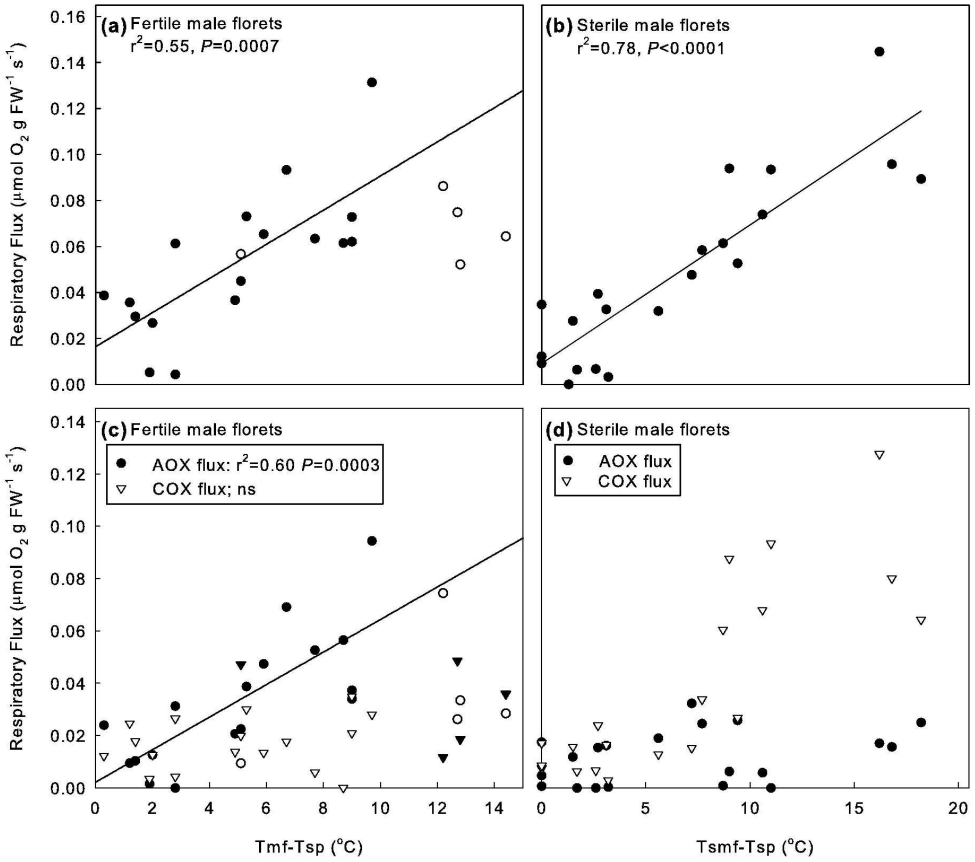

Figure 3. Relationships between total respiratory flux and heating in (a) FM florets and (b) SM florets, and between AOX (solid circles) and COX flux (open triangles) and floret heating in (c) fertile male florets and (d) sterile male florets. Heating was measured as the difference in temperature between FM florets (Tmf) or SM florets (Tsmf), and adjacent non-thermogenic spathe tissue (Tsp). Peak thermogenic stage C FM florets were excluded from correlations for both (a); total respiration (open circles) and (c); AOX (open circles) and COX fluxes (closed triangles). The regression equations are included in the text. Correlations between COX and AOX fluxes and heating not shown for SM florets due to potential diffusional limitation of isotope fractionation in air.
159x147mm (600 x 600 DPI)

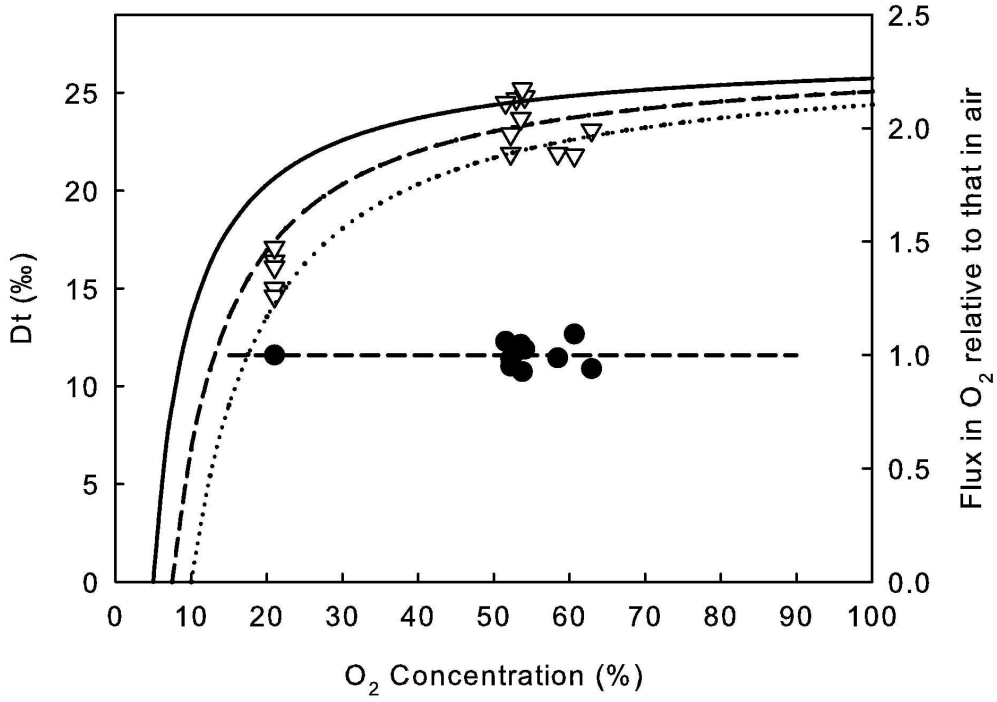

Figure 4. Theoretical discrimination (Dt; lines) as a function of external O2 (%) determined from equation 2 and using Dr=27.1 (discrimination endpoint for AOX measured under elevated O2). Pi/Pa was calculated using Pi/Pa=(Pa-G)/Pa, where G is the diffusion gradient, which was assumed to remain constant as there was no change in respiration rate as O2 was increased above 21%, as shown by the relative flux rates (closed circles) which vary little from 1 (horizontal line; mean ± SD, 1.0 ± 0.05). Dt response curves are shown for diffusion gradients (G) of 5.0% (solid line), 7.5% (dashed line) or 10% (dotted line). Using G=7.5% gave the best fit for the actual isotopic discrimination data (Dt) for stage C SM florets (open triangles). For Dt measurements, n=15 floret samples from 5 inflorescences.
159x125mm (600 x 600 DPI)

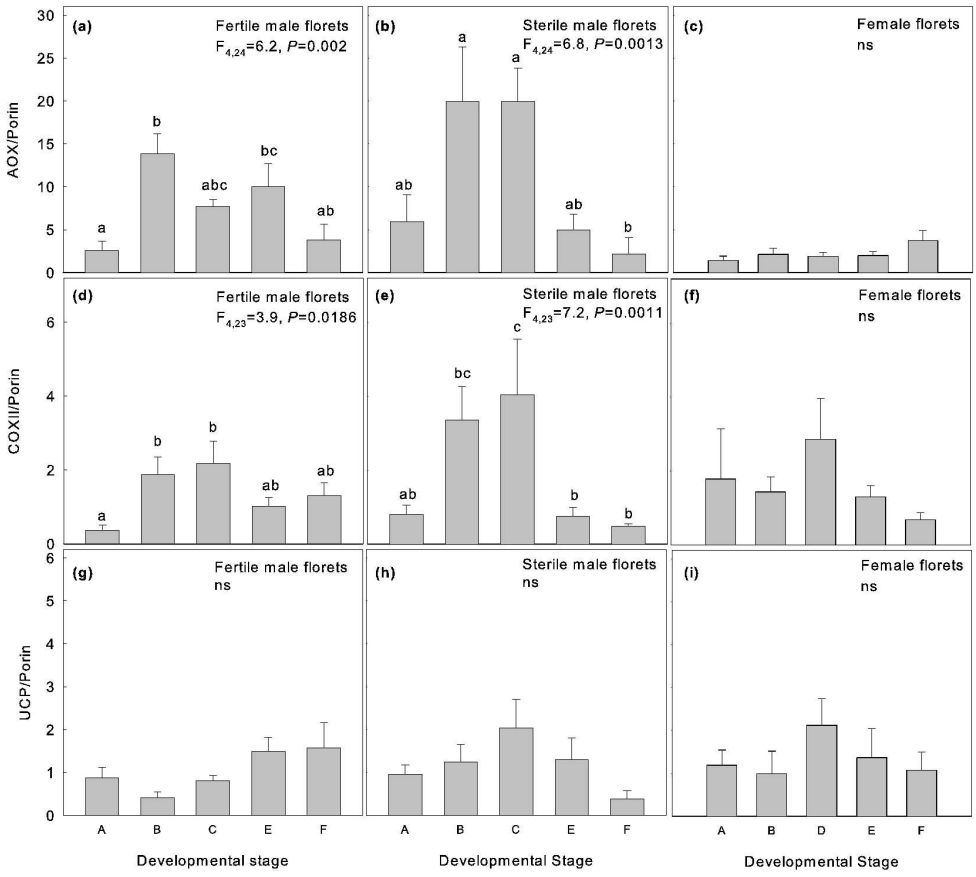

Figure 5. Densitometry results of chemiluminescent signals from western blots of AOX (a, b, d), COXII (d, e, f) and pUCP (g, h, i) proteins presented relative to Porin in fertile male florets (left panels), sterile male florets (centre panels) and female florets (right panels) of Philodendron bipinnatifidum during development. Developmental stages: A pre-thermogenesis, B shoulder, C peak, E plateau, F post-thermogenesis (refer to Fig. 1a for details). Different letters indicate significant differences between stages at P<0.05. Data are means ± SE of n=3-6 samples.
216x200mm (600 x 600 DPI)

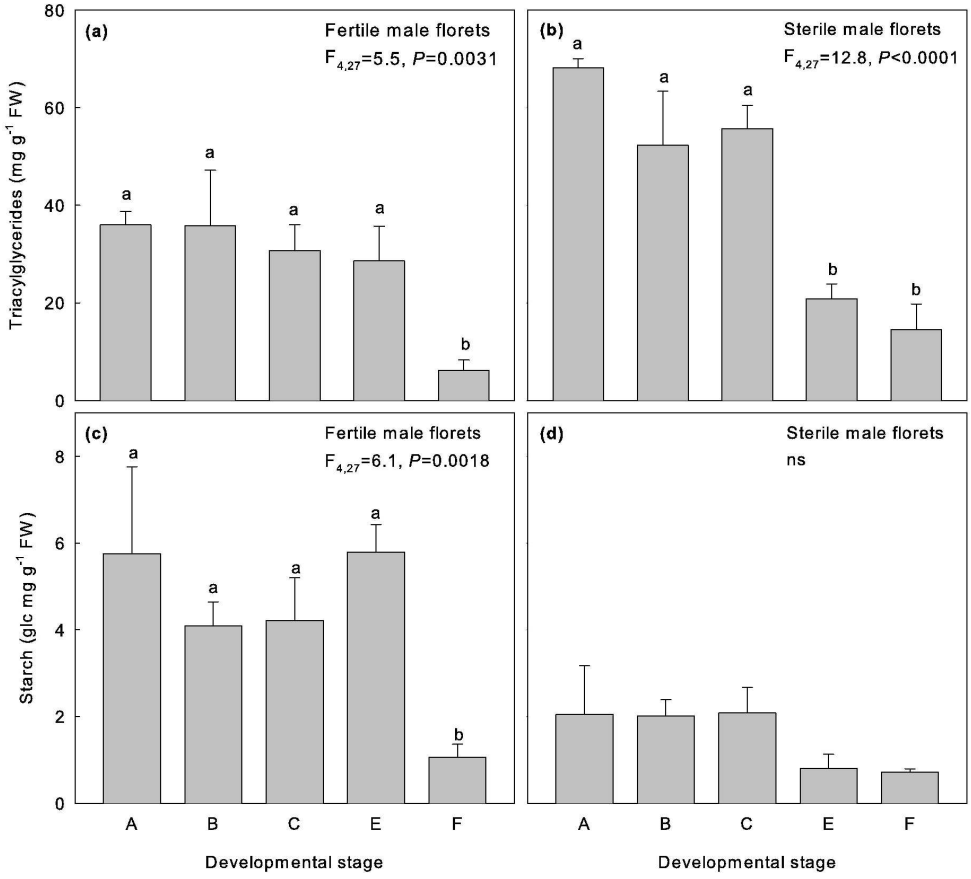

Figure 6. Changes in total triacylglyceride content (a, b), and starch content (c, d) in fertile (left panels) and sterile (right panels) male florets of Philodendron bipinnatifidum during development. Developmental stages: A pre-thermogenesis, B shoulder, C peak, E plateau, F post-thermogenesis (refer to Fig. 1a for details). Different letters indicate significant differences between stages at P<0.05. Data are means ± SE of n=4-6 samples.
159x143mm (600 x 600 DPI)